J. Braz. Chem. Soc., Vol. 13, No. 2, 200-206, 2002.
Printed in Brazil - ©2002 Sociedade Brasileira de Química
0103 - 5053 $6.00+0.00

Article

Synthesis and Structural Studies of Er^{3+} Containing Lead Cadmium Fluoroborate Glasses and Glass-Ceramics

Maurício A.P. Silva[a,b,c], Younes Messaddeq[a], Valerie Briois[b], Marcel Poulain[c] and Sidney J. L. Ribeiro*[a]

[a]*Instituto de Química, Universidade Estadual Paulista, CP 355, 14801-970, Araraquara - SP, Brazil*

[b]*LURE, Bât. 209-d, Université Paris-Sud, BP 34, 91898 Orsay-Cedex, France*

[c]*CEMA, Université de Rennes I, 35042 Rennes, France*

A partir de resultados de experimentos de fusão e choque térmico, o domínio vítreo foi identificado no sistema PbF_2-CdF_2-B_2O_3. Vidros puros e dopados com Er^{3+} foram preparados e vitrocerâmicas foram obtidas a partir de tratamentos térmicos adequados. A fase cristalina foi identificada como β-PbF_2. Estudos estruturais foram efetuados por difração e absorção de raios X e o papel desempenhado pelos átomos de Pb^{2+} e Cd^{2+} na estrutura vítrea foi estabelecido a partir destas técnicas. Os resultados sugerem que, com a cristalização, os íons Er^{3+} são segregados na fase cristalina.

The vitreous domain was established in the PbF_2-CdF_2-B_2O_3 system from melting and quenching experiments. Er^{3+} containing glasses were prepared and glass ceramics were obtained by selected heat-treatments. Lead fluoride was identified (β-PbF_2) as the crystalline phase. Structural studies were performed in some glassy and partially crystallized samples by means of X-ray Diffraction (XRD) and Extended X-ray Absorption Fine Structure (EXAFS) measurements. The role of Cd^{2+} and Pb^{2+} atoms on the glass network formation and also on the crystallization behavior was put forward by these techniques. After crystallization Er^{3+} atoms segregated in the crystal phase.

Keywords: oxifluoride glasses, glass-ceramics, x-ray absorption spectroscopy

Introduction

In the last years a new class of oxifluoride glasses have been studied aiming at the development of new photonic devices. In mixed systems involving well known glass former oxides such as SiO_2 and GeO_2 and heavy metal fluorides, stable glasses have been prepared at ambient atmospheres by melting and casting techniques.[1,2] Besides being stable and workable, *e.g.* as optical fibers and thin films, these glasses present interesting crystallization characteristics. It is possible to control the crystallization process in order to obtain transparent glass ceramics, where heavy metal nanocrystals are grown in the glassy oxide matrix. Moreover, when doped with optically active rare earth ions, these ions concentrate in the crystalline phase after the ceramization heat treatment. In parallel, similar oxyfluoride glasses display interesting ionic conduction properties.

Haloborate and halosilicate glasses have been studied and show interesting anionic conductivity properties.[3,4] Haloborate glasses in the B_2O_3-PbO-PbF_2 and B_2O_3-PbO-PbF_2-AlF_3 systems have been characterized by Raman scattering and X-ray photoelectron spectroscopy.[4] Ionic conductivity increases with the PbF_2 content. The structure of these glasses comprises discrete and polymerized structures displaying sp^2-hybridized boron and fluorine atoms bonded to B, Al and also Pb atoms.

In this work we have prepared and characterized new glasses in the B_2O_3-PbF_2-CdF_2 system. Characterization techniques include thermal analysis, X-ray diffraction and Extended X-ray Absorption Fine Structure (EXAFS). Undoped and Er^{3+}- doped samples of a selected composition were submitted to crystallization treatments and the samples were characterized by the above mentioned techniques and also by luminescence spectroscopy.

Experimental

Glasses in the B_2O_3-PbF_2-CdF_2 system were prepared by melting starting mixtures at 800 °C, in Pt crucibles,

* e-mail: sidney@iq.unesp.br

followed by quenching and casting the melts in brass molds (the cooling rate was estimated to be of the order of 10^3 K min^{-1}). Short melting times (typically 5 min) were used in order to decrease fluorine losses. Due to the low viscosity of the melt, good homogenization was easily achieved by crucible agitation before casting. Starting reagents were CdF_2 (Aldrich, 99%), orthorhombic a-PbF_2 (Aldrich, 99.99%) and H_3BO_3. Glasses with composition (mol %) $40B_2O_3$-$30PbF_2$-$30CdF_2$ were also prepared containing 1mole% ErF_3 prepared by fluorination of Er_2O_3 (Aldrich p.a.)

The glasses were then submitted to heat treatments at temperatures near the onset of crystallization, identified form thermal analysis (T_x), in order to verify the crystallization behavior of the related glass ceramics. Table 1 shows the labels used to identify the samples studied, time and temperature employed for each heat treatment. Table 2 gives the chemical analyses results obtained by ICP-AES technique for undoped $40B_2O_3$-$30PbF_2$-$30CdF_2$ glass (B sample) and corresponding heat-treated material (BT2 sample).

Thermal analyses was performed in a Thermal Analyst 3100 calorimeter from TA Instruments, under N_2 atmosphere. Characteristic temperatures Tg (glass transition temperature), Tx and Tp (onset and maximum of the crystallization peak, respectively) were obtained from DSC scans obtained with powdered samples heated at a constant heating rate q=10 K min^{-1}. X-ray powder diffraction was performed in a D-5000 Siemens diffractometer with Cu K_a radiation at 0.02° s^{-1} scanning rate.

Short range order in the samples identified in Table 1 was studied by means of Extended X-ray Absorption Fine Structure (EXAFS). Measurements were performed at the Cd K and Pb L_{III} edges, in the transmission mode, at the D44 beamline of the DCI storage ring (which works with a positron beam energy of 1.85 GeV) at LURE, France. During data collection the average current in the storage ring was 250 mA. For the Cd K-edge (26711 eV) measurements, a two-crystals Ge(400) monochromator and two krypton-filled ionization chambers were used. Spectra were obtained with an energy step of 4 eV and a counting time of 2 s. In the Pb L_{III}-edge (13035 eV) measurements, the ionization chambers were filled with argon and a two-crystals Si(111) monochromator was used. A step size of 3 eV per 2 s was employed for spectra recordings. CdF_2 (cubic) and β-PbO (orthorhombic) were used as reference compounds in the X-ray absorption experiments. Measurements were performed at the liquid nitrogen temperature (77K), in order to reduce the thermal factor, which produces a broadening of EXAFS oscillations.

Near infrared Er^{3+} emission spectra were obtained with a Spex Fluorolog spectrofluorimeter equipped with a North Coast Ge detector. Excitation was performed with a 450W Xe lamp.

Results

Glasses were obtained in the form of yellowish transparent monoliths of approximately 20x10x2 mm. The samples transparency, the typical amorphous X-ray diffraction pattern and the detection of glass transition in DSC (Differential Scanning Calorimetry) measurements identified glass formation.

The vitreous domain diagram for the ternary B_2O_3-PbF_2-CdF_2 system is illustrated in Figure 1. Glass forming compositions (under the above-cited heating-quenching conditions) are represented in this figure by open circles, while the black ones represent compositions that crystallize under the same conditions. Binary composition B_2O_3-PbF_2 was previously studied by Gressler *et al*.[5] In the ternary diagram, the composition limits for glasses in the lead cadmium fluoroborate system, expressed in mole %, are 20-60% B_2O_3, 30-60% PbF_2 and 0-50% CdF_2.

Table 3 gives the characteristic temperatures obtained from DSC measurements for some typical compositions in this system. The value obtained for the difference (Tx-Tg)

Table 1. Denomination of the samples studied

Composition	Glass (as quenched)	Annealed (470 °C/20min)	Annealed (470 °C/60min)
$40B_2O_3$-$30PbF_2$-$30CdF_2$	B	BT1	BT2
$(40B_2O_3$-$30PbF_2$-$30CdF_2)_{0.99}(ErF_3)_{0.01}$	BEr	BErT1	BerT2

Table 2. Composition of B samples obtained from ICP analysis

Nominal Composition	B sample (ICP/AES)	BT2 sample (ICP/AES)
$B_{2.7}O_4Pb_1Cd_1F_4$	$B_{1.8}O_{4.4}Pb_1Cd_1F_{1.3}$	$B_{1.8}O_{4.3}Pb_1Cd_1F_{1.3}$

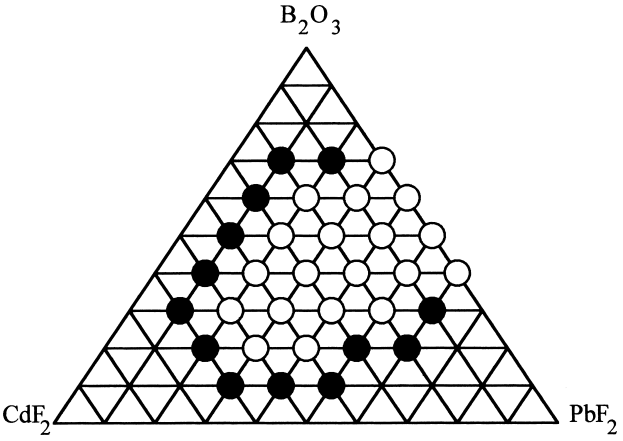

Figure 1. Vitreous domain diagram for the B_2O_3-PbF_2-CdF_2 system; black circles: crystal; white circles: glass. The experimental conditions are described in the text

Table 3. Characteristic temperatures obtained from DSC curves (Tg: glass transition temperature; Tx: onset of the crystallization exotherm; Tp: maximum of the crystallization exotherm)

Composition	Tg(ºC)	Tx(ºC)	Tp(ºC)	Tx-Tg(°C)
$50B_2O_3$-$40PbF_2$-$10CdF_2$	372	-	-	-
$45B_2O_3$-$35PbF_2$-$20CdF_2$	356	516	530	160
$40B_2O_3$-$30PbF_2$-$30CdF_2$	360	509	538	149
$35B_2O_3$-$25PbF_2$-$40CdF_2$	372	495	514	123
$30B_2O_3$-$20PbF_2$-$50CdF_2$	357	450	469	93

is usually taken as a stability parameter. With the increase in the heavy metal content a decrease is observed for (Tx-Tg). It must be noted that no crystallization could be identified for the sample with composition (mole%) $50B_2O_3$-$40PbF_2$-$10CdF_2$ in the temperature range scanned (50-600 ºC). ICP-AES technique results (Table 2) shows that, in spite of short melting time, fluorine and boron losses were not completely avoided.

Figure 2 shows the X-ray diffraction patterns of the undoped and Er-doped glassy and crystallized $40B_2O_3$-$30PbF_2$-$30CdF_2$ samples. Peaks marked with circles are those reported on the 6-0251 JCPDS file for the cubic lead fluoride β-PbF_2. This cubic phase arises from heat treatment of the glassy samples at 470 °C. In the erbium-doped sample such crystallization occurs after a shorter time heat treatment (20 min, BErT1) compared to the undoped one (60 min, BT2). The diffraction peaks of Er-doped samples is shifted to higher angles, compared to the same peaks in undoped glass-ceramics, indicating that erbium atoms are enclosed in a solid solution of the type β-PbF_2:Er^{3+}, in which Pb^{2+} ions, with an ionic radius of 0.145 nm, are partially substituted by Er^{3+} ions with ionic radius of 0.114 nm. Despite of the weak intensity of the peaks, one can observe for the BT2 and BErT2 samples some less intense peaks, marked with circles in Figure 2. We assign these peaks to the occurrence of a non-random cationic arrangement in the cadmium glassy network. This interpretation is supported by EXAFS results at the Cd K-edge, as discussed below.

EXAFS formalism and data analysis are largely described in a number of books, reviews and papers. As an example, the reader will find in reference 6 a detailed description of EXAFS phenomena and data analysis. In this work, data analysis was performed on a Macintosh computer with the A. Michalowicz's "Exafs pour le Mac" software.[7] The main steps of analysis procedure are:

1. Subtraction of absorption background by a linear function from the rough absorption data.

2. Calculation of EXAFS signal using the Lengeler-Eisenberger method[8] and its conversion to a function of wave vector $k\chi(k)$.

3. Data are then Fourier transformed, using k^3 ponderation and a Kaiser window with τ=2.5, leading to a spectrum scaled in distances (Å).

4. The peaks in the Fourier transforms corresponding to a coordination shell are filtered and back-transformed to *k*-space.

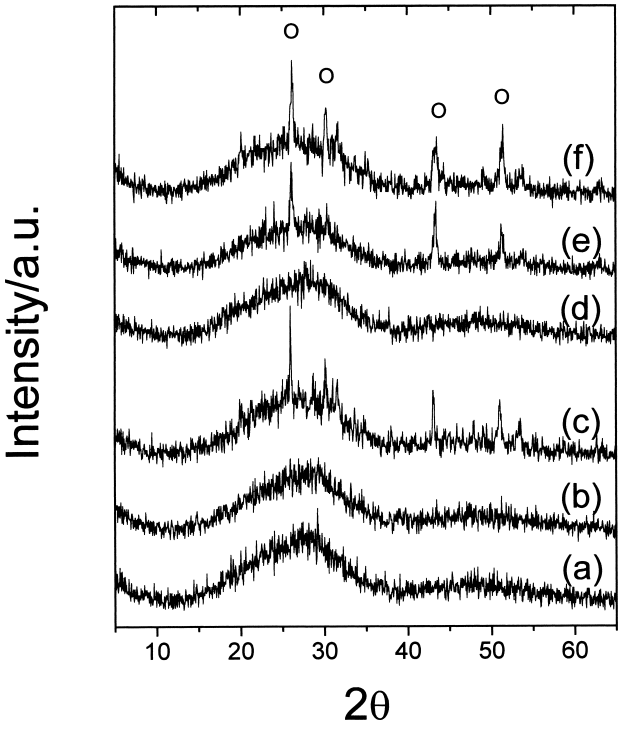

Figure 2. X-ray diffraction patterns of the undoped glasses with composition $40B_2O_3$-$30PbF_2$-$30CdF_2$: (a) as quenched, (b)- treated at 470 ºC/20 min and (c) treated at 470 ºC/60 min and of the Er-doped glasses: (d) as quenched, (e) treated at 470 ºC/20 min and (f) treated at 470 °C/60 min. Diffraction peaks marked with a circle denote the β-PbF_2 crystalline phase. Other peaks refer to a non-random cationic arrangement in the cadmium glassy network

5. The resulting EXAFS-filtered signal is treated as a sum of sinusoidal wave functions using plane wave and single scattering approximations.[6]

$$k\chi(k) = S_0^2 \sum_i \frac{N_i}{R_i^2} e^{-2k^2\sigma_i^2} e^{-\frac{2R_i\Gamma}{k}} f_{ij}(\pi,k)\sin\left[2kR_i + \Phi_i(k)\right] \quad (1)$$

where N is the number of atoms in the coordination shell, R_i is the average interatomic distance between the absorbing atom and the back scatterer atoms, σ_i is the Debye-Waller factor, which takes into account the static and thermal structural disordering, $\lambda(k)$ is the photoelectron mean free path ($\beta = k/G$), and $f_{ij}(\pi,k)$ and $\Phi_i(k)$ are the amplitude and the phase functions for this coordination shell. In the case of Pb L_{III}-edge studies, amplitude and phase functions were calculated from McKale tables[9] after checking on the β-PbO reference compound. These amplitude and phase functions are applied in the simulation of the first coordination shell of the standard orthorhombic PbO compound, in order to test these theoretical functions and calculate the mean free path constant Γ, determined as 1.22 $Å^{-2}$ for the first oxygen coordination shell. At the Cd K-edge, these functions were obtained experimentally from the reference compound CdF_2. It crystallizes in the cubic form, following the face centered cubic (FCC) pattern in which cadmium atoms have the first coordination shell composed by 8 fluorine atoms at 2.33Å.[10]

6. Finally, a least square fitting is implemented on the Fourier-filtered signal obtained for the glasses and glass ceramics, leading to the determination of the structural parameters R, N and σ, corresponding to the respective coordination shells of the absorbing atoms.

The reliability of the fit is given by:

$$\rho = \frac{\sum_i k_i \left[\chi_{\exp}(k_i) - \chi_{th}(k_i)\right]^2}{\sum_i k\chi_{\exp}(k_i)^2} \quad (2)$$

Figure 3 shows the resulting |F(r)| curves of the EXAFS spectra obtained at the Cd K-edge for the samples. Samples B, BT1, BEr and BErT1 present only one peak located at about 1.8 Å (uncorrected for phase shift), related to the first coordination shell around cadmium atoms (composed by light atoms like fluorine or oxygen). The second peak (centered at about 3.15Å, uncorrected for phase shift), observed in samples BT2 and BErT2, indicates that some cationic ordering occurs at medium range distance, in the second Cd coordination shell.

The first peak in the |F(r)| curve of the samples was filtered between 1.11 and 1.30Å and back-transformed to k ($Å^{-1}$) space before being fitted by a shell of light atoms.

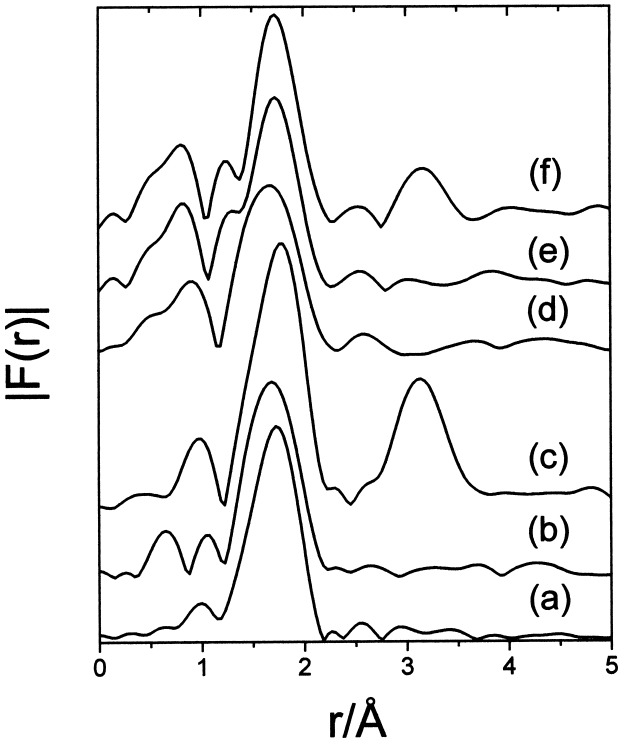

Figure 3. Fourier transform |F(r)| curves obtained from the filtered EXAFS spectra (Cd K-edge). Undoped glass: (a) as quenched, (b) treated at 470 °C/20 min and (c) treated at 470 °C/60 min. Er^{3+} doped glasses: (d) as quenched, (e) treated at 470 °C/20 min and (f) treated at 470 °C/60 min

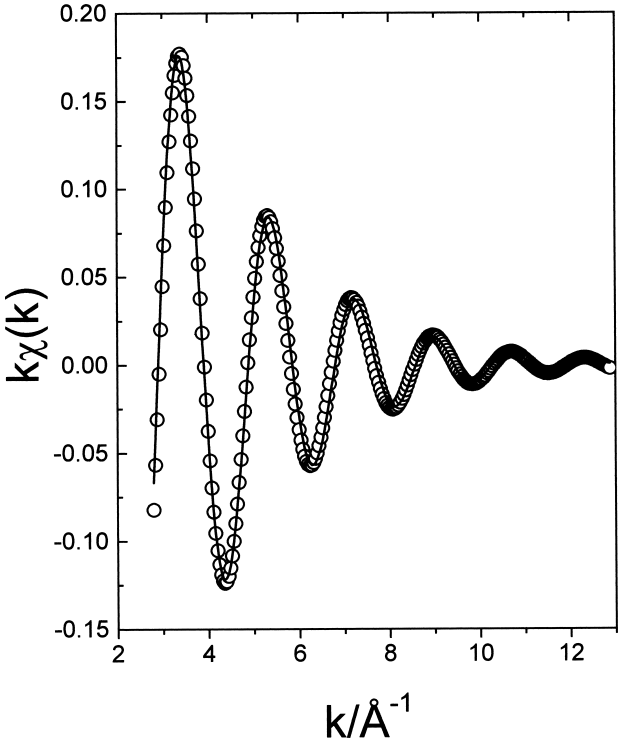

Figure 4. EXAFS spectra. Simulation of the first coordination shell for sample B (undoped glass as quenched. Cd K-edge). Circles: experiment; continuous line: simulation

Figure 4 illustrates, as an example, the fit of this signal obtained for the B sample and Table 4 gives the structural parameters so obtained using phase and amplitude functions related to fluorine atoms. Due to close electronic structures, similar results can be obtained by using phase and amplitude functions related either to fluorine or oxygen atoms. Therefore, we are unable to differentiate between fluorine and oxygen in the first coordination shell. We adopt the general term "anions" for the first neighbors of cadmium. In glassy and glass-ceramic samples, quantitative simulation of the first coordination shell gives 4.2±0.4 anions at about 2.25±0.01Å.

The Fourier transforms of the EXAFS curves obtained at the Pb L_{III}-edge for the same samples are presented in Figure 5. Splitting of the first peak is observed for all the samples. Moreover a second broad band in the R-space between 4-5 Å is observed for samples BT2, BErT1 and BErT2. As discussed elsewhere[11] the occurrence of such splitting in the first peak of the |F(r)| curves of EXAFS spectra obtained at the Pb L_{III}-edge is related to a multi-shell environment with a large distance distribution in each sub-shell. Considering those results, a multi-shell fitting procedure was used and numerical results are reported in Table 5, with an example of fit in Figure 6 for B sample. Results gathered in Table 5 suggest a first coordination shell around the lead atoms composed by anions (fluorine and/or oxygen atoms)

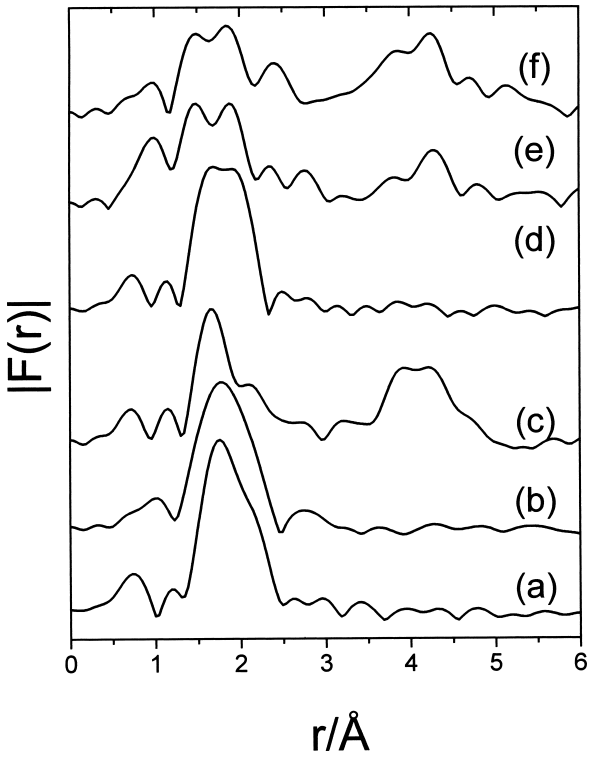

Figure 5. Fourier transform |F(r)| curves obtained from the filtered EXAFS spectra (Pb L_{III}-edge). Undoped glass: (a) as quenched, (b) treated at 470 °C/20 min and (c) treated at 470 °C/60 min. Er^{3+} doped glasses: (d) as quenched, (e) treated at 470 °C/20 min and (f) treated at 470 °C/60 min

Table 4. EXAFS results obtained at the Cd K-edge (N: number of atoms; R: mean distance; σ: Debye Waller factor; ΔE_0: energy shift; ρ: fit reliability)

	B	BT1	BT2	BEr	BErT1	BerT2
N	4.0	4.1	4.6	4.0	3.8	4.1
σ (Å)	0.092	0.096	0.084	0.097	0.091	0.094
R (Å)	2.24	2.25	2.26	2.25	2.24	2.25
ΔE_o(eV)	0.0	0.2	1.9	1.5	0.2	0.8
ρ	$7.5x10^{-3}$	$2.6x10^{-3}$	$3.6x10^{-3}$	$4.8x10^{-3}$	$3.8x10^{-3}$	$2.5x10^{-3}$

Table 5. EXAFS results obtained at the Pb L_{III}-edge (N: number of atoms; R: mean distance; σ: Debye Waller factor; ΔE_0: energy shift; ρ: fit reliability)

	B	BT1	BT2	BEr	BErT1	BerT2
N	1.4	1.8	1.4	1.6	1.8	1.3
	2.0	2.3	2.6	3.4	3.0	2.8
			2.7		3.3	3.2
σ (Å)	0.091	0.114	0.108	0.106	0.124	0.147
	0.109	0.116	0.133	0.158	0.167	0.144
			0.178		0.192	0.152
R (Å)	2.24	2.23	2.24	2.29	2.25	2.27
	2.40	2.38	2.40	2.39	2.36	2.35
			2.56		2.58	2.57
ΔE_o(eV)	6.5	2.8	0.6	3.7	1.2	-0.1
	10.3	5.9	3.9	5.9	6.1	4.3
			10.8		8.7	8.7
ρ	$1.2x10^{-3}$	$2.3x10^{-3}$	$2.7x10^{-3}$	$2.9x10^{-3}$	$2.4x10^{-3}$	$2.9x10^{-3}$

into two sub-shells centered at about 2.25±0.02Å and 2.38±0.02Å. As detected by X-ray diffraction, crystallization of cubic lead fluoride in BT2, BErT1 and BErT2 samples was also evidenced from EXAFS analysis. In cubic lead fluoride, λ-PbF_2, the distance between the central lead atom and its first eight-fold fluorine coordination shell is 2.57Å. In samples BT2, BErT1 and BErT2 a third sub-shell of anions at 2.57±0.01Å is necessary to simulate satisfactorily the first Pb coordination shell (Table 5).

Figure 7 shows Er^{3+} infrared emission spectra obtained under excitation at 378nm (Er^{3+} $^4I_{15/2}\rightarrow{}^4G_{11/2}$ absorption transition). The $^4I_{13/2}\rightarrow{}^4I_{15/2}$ transition is observed with the typical inhomogeneously broadened spectrum, due to the statistical distribution of sites for the base glass (Figure 7(a)). After heat treatment some well resolved lines are clearly observed (Figure 7(b)). Figure 7(c) shows the spectrum obtained for a lead fluorogermanate transparent glass-ceramic[2] for comparison purposes.

Discussion

Very stable glasses were obtained in this system. Despite the fact that it is not the scope of this paper, the possibility of fiber drawing from the undercooled melt of several glassy compositions was observed. Sample B, with composition (in mole%) $40B_2O_3$-$30PbF_2$-$30CdF_2$, is a typical example of those observations. The (Tx-Tg) difference, which expresses the temperature range in which the undercooled melt can be worked without any appreciable crystallization, is 149 °C (Table 3). The composition of the samples studied by DSC does not allow a direct comparison of glass transition temperatures. In fact, when the fluorine content increases (fluorine anions are considered non-bridging, and thus reduce the network connectivity and decrease Tg) the concentration of lead atoms decreases (heavy cations acting as modifiers also decrease Tg). These two associated processes do not allow a continuous variation in Tg with the compositions studied.

Crystallization of β-PbF_2 in heat-treated samples was evidenced both by X-ray diffraction and EXAFS measurements. X-ray absorption results have revealed, not only the role played by lead atoms in glass-ceramic formation, but also the network former character of cadmium atoms. Indeed, as in the case of fluorosilicate glasses and glass-ceramics,[12] a four-fold coordination shell around cadmium atoms, together with a drastic shortening of interatomic distance (2.25Å) compared with the crystalline CdF_2 (2.33Å) are observed for fluoroborate glasses. We assume that the change in cadmium environment in the glass, compared to CdF_2, results from the loss of boron and fluorine

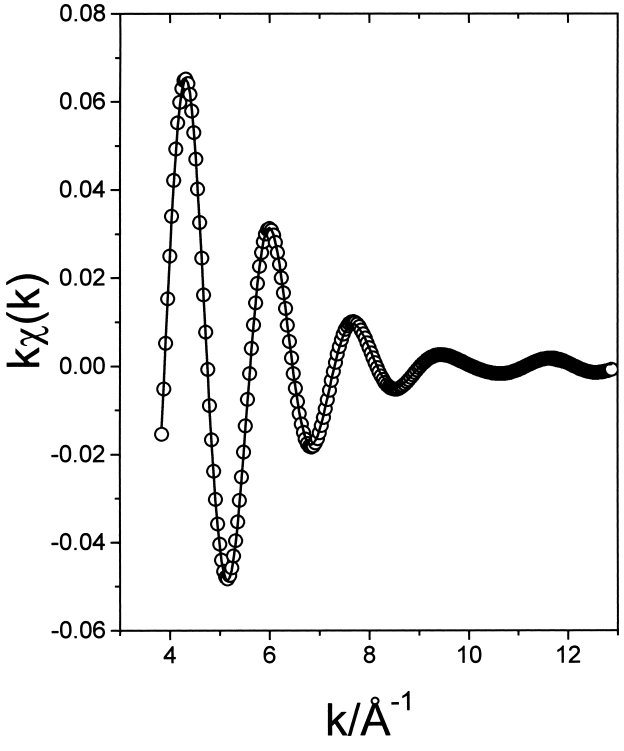

Figure 6. EXAFS spectra. Simulation of the first coordination shell for the sample B (Undoped glass as quenched. Pb L_{III}-edge). Circles: experiment; continuous line: simulation

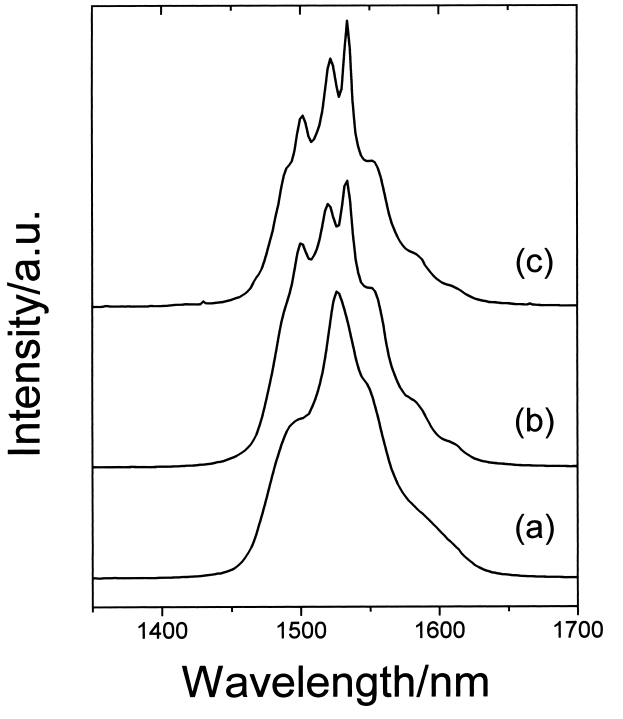

Figure 7. Room temperature Er^{3+} emission spectra (λ_{EXC}=378 nm) obtained for (a) glass BEr; (b) glass-ceramic BErT2 and (c) lead fluorgermanate transparent glass-ceramic[2]

atoms during the glass preparation (Table 2) following upon the formation of BF_3. The resulting excess of oxygen atoms could form an oxygen-fluorine anionic network around the cadmium cations. The peak at about 3.1Å (uncorrected for phase shift) in the BT2 and BErT2 samples reflects some cationic ordering in the second Cd coordination shell upon heating. The weak-intensity diffraction peaks observed in Figure 2 support this assumption. It is noteworthy that this thermal behavior is opposite to the one observed with the fluorosilicate system,[12] for which no medium range ordering was observed after heating.

Pb L_3-edge EXAFS results show clearly the role played by lead atoms in glassy network building and crystallization behavior of glass-ceramics. In glasses B and BEr and in the heat treated sample BT1 we have found a first coordination shell around lead atoms composed by anions presenting a distance distribution centered around 2.25 and 2.38Å. These mean distances were also observed for $PbO\text{-}SiO_2$ glasses by Imaoka *et al.*[13] After heat treatment samples BT2, BErT1 and BErT2 present, in addition to these shorter distances, anions at 2.57Å, characteristic of $\beta\text{-}PbF_2$.

Diffraction results give important information about erbium during crystallization. The diffraction peaks related to the cubic lead fluoride appear, in samples BErT1 and BErT2, shifted to higher angles by comparison to the ones in sample BT2. This contraction of the lattice parameter of the $\beta\text{-}PbF_2$ phase caused by erbium atoms indicates the inclusion of the rare earth in the crystalline phase.

After heat treatment a portion of lead atoms remain in the glassy matrix as evidenced by the simulation of the first coordination shell in Table 5. Compared to the fluorosilicate system,[11] $\beta\text{-}PbF_2$ crystallization is less efficient for fluoroborate system studied herein.

The spectroscopic characteristics shown in Figure 7 give a clear indication that after heat treatment Er^{3+} ions are located in a crystalline environment. Some of us[2] have shown that the spectrum displayed in Figure 7(c), obtained for the $PbGeO_2\text{-}CdF_2\text{-}PbF_2$ system, could be assigned to Er^{3+} doped $\beta\text{-}PbF_2$ crystals. The same spectral shape observed in Figures 7 (b) and (c) suggests that the same reasoning could be claimed here, corroborating XRD and EXAFS results shown above.

Conclusion

Stable glasses have been obtained for the $B_2O_3\text{-}PbF_2\text{-}CdF_2$ system and the ternary glassy domain diagram was determined. Glass ceramics were obtained by annealing at 470 °C, with $\beta\text{-}PbF_2$ as the main crystalline phase. Structural studies on glasses and glass-ceramics outline the role played by cadmium and lead atoms in glass formation and crystallization. Cadmium appears four-fold coordinated, preferentially by oxygen atoms. CdO_4 units participate in glassy network building but, during crystallization, clusters of non-disordered anionic arrangements are observed. Lead environment, as determined by EXAFS studies, consists of oxygen and fluorine anions at different distances. Spectroscopic measurements combined with EXAFS and XRD results suggest that Er^{3+} ions are incorporated in the cubic $\beta\text{-}PbF_2$ phase.

Acknowledgments

Financial support from FAPESP, CNPq and PRONEX (Brazilian Agencies) is acknowledged. M. A. P. Silva acknowledges also CAPES/COFECUB for a PhD grant.

References

1. Beall, G. H.; Pinckney, L. R.; *J. Am. Ceram. Soc.* **1999**, *82*, 5.
2. Bueno, L. A.; Melnikov, P.; Messaddeq, Y.; Ribeiro, S. J. L.; *J. Non-Cryst. Solids* **1999**, *247*, 87.
3. Coon, J.; Horton, M.; Shelby, J.E.; *J. Non-Cryst. Solids* **1988**, *102*, 143.
4. Wang, Y.; Osaka, A.; Miura, Y.; *J. Non-Cryst. Solids* **1989**, *112*, 323.
5. Gressler, C. A.; Shelby, J. E.; *J. Appl. Phys.* **1989**, *66*, 3.
6. Teo, B. K.; *EXAFS: Basic Principles and Data Analysis*, Inorg. Chem. Concepts vol. 9, Springer: Berlin, 1986.
7. Michalowicz, A.; *EXAFS pour le Mac*, Societé Française de Chimie: Paris, 1991, p. 102.
8. Lengeler, B.; Eisenberger, P.; *Phys. Rev. B* **1980**, *21*, 4507.
9. McKale, A. G.; Veal, B. W.; Paulikas, A.,P.; Chan, S.,K.; Knapp, G.S.; *J. Am. Chem. Soc.* **1988** *110*, 3763.
10. Wyckoff, R.W.; *Crystal Structures*, 2nd ed., R. E. Krieger Publishing Company: Malabar, Florida, 1982, vol. 1, p. 241.
11. Silva, M. A. P.; Poulain, M.; Villain, F.; Briois, V.; Ribeiro, S. J. L.; Messaddeq, Y.; *J. Phys. Chem. Solids* **2001**, *62*, 1055.
12. Silva, M. A. P.; *Ph.D. Thesis*, Universidade Estadual Paulista Júlio de Mesquita Filho, Brazil, 2000.
13. Imaoka, M.; Hasegawa, H.; Yasui, I.; *J. Non Cryst. Solids* **1986**, *85*, 393.

Received: February 9, 2001
Published on the web: February 14, 2002

FAPESP helped in meeting the publication costs of this article.